The discrete Swift-Hohenberg equation

Lambertus A. Peletier & José Antonio Rodríguez

1 Introduction

In the study of pattern formation the *Swift-Hohenberg equation*,

$$\frac{\partial u}{\partial t} = \alpha u - \left(1 + \frac{\partial^2}{\partial x^2}\right)^2 u - u^3, \qquad 0 < x < L, \quad t > 0, \tag{SH}$$

is a classical model equation. Here, α and the length L of the domain are eigenvalue parameters. This equation is known to possess a rich structure of stationary solutions with complex graphs [9], many of them locally stable. An important issue is here the selection of patterns that develop as the system evolves to a final state. Since the Swift-Hohenberg equation is a gradient system [4, 7, 8] final states will be stationary solutions, provided they are isolated. This limits the choice to the set of equilibrium states and thus simplifies the problem to a certain extent.

However, this is still a complicated problem, and in the literature several simplified versions of the Swift-Hohenberg equation have been studied [6]. In the present paper we introduce another simplification, reducing (SH) to an equation on a finite lattice with $N+1$ nodes. We establish some properties of solutions $\mathbf{x} = (x_0, \ldots, x_N)$, keeping N general, but our main results concern the dynamics of the system when $N = 4$ and the outer nodes, x_0 and x_4, are kept fixed. This leaves a three-dimensional system of ordinary differential equations, or, in the presence of symmetries, an even lower-dimensional system, which is simple enough to understand in great detail, whilst still complex enough to show several of the properties of the original SH equation, such as the selection of different patterns as time runs to infinity. The objective of this paper is to use this simple model to shed light on the dynamics of the SH equation.

It is instructive to place the study of the Swift-Hohenberg equation against the backdrop of the *Fisher-Kolmogorov equation*

$$\frac{\partial u}{\partial t} = \frac{\partial^2 u}{\partial x^2} + u(1 - u^2), \qquad 0 < x < L, \quad t > 0, \tag{FK}$$

also a gradient system, but of second order. The dynamics of the Cauchy-Dirichlet problem for this equation was first studied in a classical study by Chafee & Infante [3]. who found that for $L \leqslant \pi^2$, the origin is a global attractor, whilst for any $L > \pi^2$ there exist two stable stationary solutions, $\pm v(x)$, where

$v(x) > 0$ for all $x \in (0, L)$. All other stationary states, and as L increases, their number also increases, are unstable. Therefore, for this equation the selection of the final pattern is quite simple.

Thus, in this paper we consider two lattice equations, one emulating the Swift-Hohenberg equation, and the other the Fisher-Kolmogorov equation. We begin with the latter, which is simpler.

Fisher-Kolmogorov equation: We first rescale the variables, putting $x = Lx^*$, $t = L^2 t^*$. This transforms the domain to the interval $(0, 1)$, and we obtain

$$u_t = u_{xx} + \sigma u(1 - u^2), \qquad 0 < x < 1, \quad t > 0, \qquad \sigma = L^2,$$

where we have dropped the asterisks again. We then replace the diffusion term by symmetric coupling of nearest neighbours, as is done in finite difference approximations, and obtain the equation

$$x_n'(t) = \Delta x_n(t) + \sigma\, f(x_n(t)), \qquad n = 1, \ldots, N-1, \tag{1.1}$$

in which Δ denotes the *discrete Laplacian operator*:

$$\Delta x_n = x_{n+1} - 2x_n + x_{n-1}. \tag{1.2}$$

Swift-Hohenberg equation: As before, we rescale the variables and put

$x = Lx^*$. This yields the equation

$$u_t = -\gamma^2 u_{xxxx} - 2\gamma u_{xx} - (1-\alpha)u - u^3, \qquad 0 < x < 1, \quad t > 0, \qquad \gamma = \frac{1}{L^2}.$$

We replace the second order derivative by the symmetric coupling term involving nearest neighbours (1.2), and the fourth order derivative by a symmetric coupling term involving the nearest– as well as the next-nearest neighbours. This results in the equation

$$u_n'(t) = -\gamma^2 \Delta^2 u_n(t) - 2\gamma \Delta u_n(t) - (1-\alpha)\, u_n(t) - u_n^3(t), \tag{1.3}$$

in which $n = 1, \ldots, N-1$, and

$$\Delta^2 u_n = u_{n+2} - 4u_{n+1} + 6u_n - 4u_{n-1} + u_{n-2}. \tag{1.4}$$

Note that the discrete Fisher-Kolmogorov equation (1.1) has one parameter, $\sigma = L^2$, whilst the discrete Swift-Hohenberg equation (1.3) has two parameters, $\alpha > 0$ and $\gamma = 1/L^2$. As was shown in [9], the number of stationary states, and the complexity of their graphs, increases as α and L increase, and hence as γ *decreases*.

Like the Swift-Hohenberg and the Fisher-Kolmogorov equation, both discrete equations are gradient systems. In the next section we define the corresponding actions J_F and J_S.

In a recent paper [7] (see also [8]) numerical simulations were made of the evolution of solution profiles of the Swift-Hohenberg equation and of the pattern selection for different values of the length L of the interval. At critical values of L, the final pattern was found to switch abruptly from one type to another, with a different number of nodes. In this paper, by studying a much simplified system, we wish to shed light on this switching phenomenon and to understand the dynamics that leads to it.

Since both discrete equations are gradient systems, limiting profiles are all stationary solutions, because they are isolated. Thus, we begin with an analysis of the equilibrium profiles. This leads to nonlinear eigenvalue problems, the eigenvalue being L for the FK-equation and γ for the SH-equation, when we keep α fixed. In Figure 1, we draw the norm of the symmetric equilibria versus the length L, first for the discrete FK equation and then for the discrete SH equation, with fixed $\alpha = 0.7$. The stable equilibria are shown with solid line and the unstable ones with dashed lines.

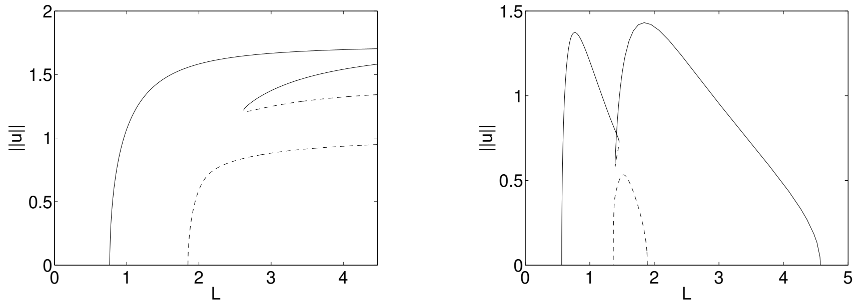

(a) Discrete FK equation.

(b) Discrete SH equation with $\alpha = 0.7$.

Figure 1: Graph of $\|\mathbf{u}\|$ versus L.

2 Preliminaries

We begin with some general properties of the discrete versions of the second order Fisher-Kolmogorov equation and the fourth order Swift-Hohenberg equation.

The discrete Fisher-Kolmogorov equation:

$$\begin{cases} u_n' = \Delta u_n + \sigma f(u_n) & n = 1, 2, \ldots, N-1, \quad t > 0, & (2.1a) \\ u_n = 0 & n = 0,\ N, \quad t > 0, & (2.1b) \\ u_n(0) = u_{n,0}, & n = 1, 2, \ldots, N-1, & (2.1c) \end{cases}$$

Here, Δ denotes the discrete Laplacian operator defined in (1.2), the parameter

σ is positive, and the function f as given by

$$f(s) = s - s^3. \tag{2.2}$$

Let us introduce some notation. We will denote vectors in $\mathbb{R}^{N-1}$ by $\mathbf{u}$, and given a function f defined from $\mathbb{R}$ to $\mathbb{R}$, we will write

$$\mathbf{f}(\mathbf{u}) = \big(f(u_1), f(u_2), \ldots, f(u_{N-1})\big)^T.$$

With this notation equation (2.1a) can be rewritten as

$$\mathbf{u}'(t) = -A\mathbf{u}(t) + \sigma\mathbf{f}(\mathbf{u}), \tag{2.3}$$

where $A = (a_{ij})$ is the symmetric positive definite matrix with $a_{jj} = 2$ and $a_{j,j+1} = -1$, $a_{j+1,j} = -1$, and all other entries equal to 0. Its eigenvalues λ_j are given by $2\big(1 - \cos(\frac{\pi j}{N})\big)$ for $j = 1, \ldots, N-1$. Note that for $\sigma = 0$, the system (2.1) is linear and that the solution is given by

$$\mathbf{u}(t) = e^{-At}\,\mathbf{u}(0), \tag{2.4}$$

where $\mathbf{u}(0) = (u_{1,0}, \ldots, u_{N-1,0})^T$. Since $\lambda_j > 0$ for $j = 1, \ldots, N-1$, the origin is asymptotically stable.

Associated with equation (2.1) we define the *Action*

$$J_F(\mathbf{u}) \stackrel{\text{def}}{=} J_1(\mathbf{u}) - \sigma \sum_{n=1}^{N-1} F(u_n), \tag{2.5}$$

in which

$$J_1(\mathbf{u}) \stackrel{\text{def}}{=} \frac{1}{2}\mathbf{u}^T A\mathbf{u} = \frac{1}{2}\sum_{n=1}^{N}(u_n - u_{n-1})^2, \tag{2.6}$$

where $u_0 = 0$ and $u_N = 0$, and F is a primitive of f:

$$F(s) \stackrel{\text{def}}{=} \int_0^s f(t)\,dt = \frac{s^2}{2} - \frac{s^4}{4}. \tag{2.7}$$

We can write equation (2.1a) as a gradient system involving the action J_F:

$$\mathbf{u}'(t) = -\nabla J_F\big(\mathbf{u}(t)\big). \tag{2.8}$$

The discrete Swift-Hohenberg equation:

$$\begin{cases} u_n' = -\gamma^2\Delta^2 u_n - 2\gamma\Delta u_n - f_\alpha(u_n), & n = 1, \ldots N-1, \quad t > 0, \qquad \text{(2.9a)} \\ u_n = 0, \qquad \Delta u_n = 0, & n = 0,\ N, \qquad t > 0 \qquad \text{(2.9b)} \\ u_n(0) = u_{n,0}, & n = 1, \ldots N-1. \qquad \text{(2.9c)} \end{cases}$$

The operator Δ is the discrete Laplacian operator, defined in (1.2), Δ^2 is the discrete bi-Laplacian defined in (1.4) and we introduce virtual nodes at $n = -1$

and $n = N + 1$, where we define $u_{-1} = -u_1$ and $u_{N+1} = -u_{N-1}$, in order to make Δ and Δ^2 well defined at all the nodes, and ensure that $\mathbf{u}$ is odd with respect to the end points. The function f_α is given by

$$f_\alpha(s) = s^3 + (1-\alpha)s, \qquad \alpha > 0. \tag{2.10}$$

Equation (2.9a) can be rewritten as

$$\mathbf{u}'(t) = -\gamma^2 A^2 \mathbf{u}(t) + 2\gamma A\mathbf{u}(t) - \mathbf{f}_\alpha\big(\mathbf{u}(t)\big), \tag{2.11}$$

where the matrix A is as in (2.3). In general we will focus on $\alpha \in (0, 1)$ and $\gamma > 0$, although we will sometimes give results for $\alpha > 1$.

Associated with equation (2.9) we define the action

$$J_S(\mathbf{u}) \stackrel{\text{def}}{=} \gamma^2 J_2(\mathbf{u}) - 2\gamma J_1(\mathbf{u}) + \sum_{n=1}^{3} F_\alpha(u_n), \tag{2.12}$$

where F_α denotes the potential

$$F_\alpha(s) = \int_0^s f_\alpha(t)\, dt = \frac{1}{4}s^4 + \frac{1-\alpha}{2}s^2, \tag{2.13}$$

which has a single well if $\alpha < 1$ and a double well if $\alpha > 1$. The functionals J_1 (cf. (2.6)) and J_2 are defined as follows:

$$J_1(\mathbf{u}) = \frac{1}{2}\mathbf{u}^T A\mathbf{u}, \qquad J_2(\mathbf{u}) \stackrel{\text{def}}{=} \frac{1}{2}\mathbf{u}^T A^2\mathbf{u} = \sum_{n=1}^{N-1} (\Delta u_n)^2. \tag{2.14}$$

As in (2.8), we can write equation (2.9a) as a gradient system:

$$\mathbf{u}'(t) = -\nabla J_S\big(\mathbf{u}(t)\big).$$

It follows that the critical points of J_F, respectively J_S, are precisely the equilibrium states of Problems (2.1) and (2.9).

Thus, Problems (2.1) and (2.9) are gradient systems, and it is readily shown that both actions, J_F and J_S, are coercive, bounded below, and that they decrease along orbits. For both systems, finding equilibrium states can be reduced to a problem of searching for roots of a certain polynomial, a procedure which will be used in later sections of this paper. In particular, this implies that the set of equilibrium states is finite and discrete. Therefore, we may conclude [5] that every orbit tends to an equilibrium state as $t \to \infty$, i.e. for every $\mathbf{u}_0 \in \mathbb{R}^{N-1}$ there exists an equilibrium state $\mathbf{u}_\infty = \mathbf{u}_\infty(\mathbf{u}_0)$ such that the orbit $\mathbf{u}(t) = \mathbf{u}(t, \mathbf{u}_0)$, which starts at $\mathbf{u}_0$, tends to $\mathbf{u}_\infty$:

$$\lim_{t\to\infty} \mathbf{u}(t) = \mathbf{u}_\infty.$$

Thus, in the description of the large time behaviour of the discrete Fisher-Kolmogorov and the discrete Swift-Hohenberg equation, equilibrium solutions play a pivotal role. We therefore first focus on giving a complete characterisation of the sets of equilibrium states of these equations.

We conclude this section with a few observations about symmetry properties of solutions. We consider the following linear operators in $\mathbb{R}^{N-1}$:

$$\begin{array}{rcl} L_1(u_1, u_2, \ldots, u_{N-2}, u_{N-1}) & = & (-u_1, -u_2, \ldots, -u_{N-2}, -u_{N-1}), \\ L_2(u_1, u_2, \ldots, u_{N-2}, u_{N-1}) & = & (\ \ u_{N-1}, \ \ u_{N-2}, \ldots, \ \ u_2, \ \ u_1), \\ L_3(u_1, u_2, \ldots, u_{N-2}, u_{N-1}) & = & (-u_{N-1}, -u_{N-2}, \ldots, -u_2, -u_1). \end{array} \tag{2.15}$$

Note that $L_3 = L_1 L_2 = L_2 L_1$. The unique fixed point of L_1 is the origin, while the fixed points of the other operators are given by

$$\begin{array}{lcl} \Pi_2 & \overset{\text{def}}{=} & \left\{ \mathbf{u} \in \mathbb{R}^{N-1} : u_j = u_{N-j} \quad \text{for every } j = 1, \ldots, N-1 \right\}. \\ \Pi_3 & \overset{\text{def}}{=} & \left\{ \mathbf{u} \in \mathbb{R}^{N-1} : u_j = -u_{N-j} \quad \text{for every } j = 1, \ldots, N-1 \right\}. \end{array} \tag{2.16}$$

The operator L_1 maps each point $\mathbf{u}$ onto the symmetric point with respect to the origin, L_2 maps each point $\mathbf{u}$ onto the symmetric point with respect to the linear subspace Π_2. Finally, L_3 maps each point $\mathbf{u}$ onto the symmetric point with respect to the linear subspace Π_3.

Invariance of the flow with respect to Π_2 in the discrete model corresponds to the following property for every $t > 0$ in the continuous model.

$$u(x) = u(L - x), \qquad \text{for every} \quad x \in (0, L). \tag{2.17}$$

Similarly, invariance of the flow with respect to Π_3 in the discrete model corresponds to the following property holding for every $t > 0$ in the continuous model.

$$u(x) = -u(L - x), \qquad \text{for every} \quad x \in (0, L). \tag{2.18}$$

In the following lemma we show that the flow $\phi_t(\cdot)$ associated with either Problem (2.1) or Problem (2.9) commutes with each of the operators L_i.

Lemma 2.1 *The flows associated with Problem* (2.1) *and Problem* (2.9) *have the properties*

$$\phi_t\big(L_i(\mathbf{u})\big) = L_i\big(\phi_t(\mathbf{u})\big) \qquad \textit{for every } t > 0 \quad \textit{and} \quad i = 1, 2, 3. \tag{2.19}$$

The proof is readily given by inspection.

Points contained in Π_2 will be called *symmetric* and points contained in Π_3 will be called *antisymmetric*.

Corollary 2.1 *The sets* Π_2 *and* Π_3 *are invariant.*

Proof. Let $\mathbf{u}_0 \in \Pi$. Then $L_2(\mathbf{u}_0) = \mathbf{u}_0$ and by Lemma 2.1, $L_2\big(\phi_t(\mathbf{u}_0)\big) = \phi_t(\mathbf{u}_0)$. Therefore, $\phi_t(\mathbf{u}_0)$ is a fixed point of L_2 and hence, $\phi_t(\mathbf{u}_0) \in \Pi_2$. The proof of the invariance of Π_3 is similar. □

This corollary allows us to call solutions in Π *symmetric* and solutions in Γ *antisymmetric.*

We will show in the following sections that for $\sigma \leqslant 2$ and for $\alpha \leqslant (2\gamma - 1)^2$, the set Π_2 attracts solutions of respectively the Fisher-Kolmogorov equation and the Swift-Hohenberg equation, and that $\mathbf{u}_\infty \in \Pi_2$.

3 The discrete Fisher-Kolmogorov equation

In this section we investigate the discrete Fisher-Kolmogorov equation in a lattice consisting of 5 nodes, $u_0, \dots u_4$, of which the end nodes u_0 and u_4 are fixed and assumed to be equal to zero. For the intermediate nodes, $u_1,\ u_2$ and u_3 we then find the following system of equations

$$\begin{cases} u_1' = -2u_1 + u_2 + \sigma f(u_1), & (3.1\text{a}) \\ u_2' = u_1 - 2u_2 + u_3 + \sigma f(u_2), & (3.1\text{b}) \\ u_3' = u_2 - 2u_3 + \sigma f(u_3). & (3.1\text{c}) \end{cases}$$

We will be studying the evolution of the solution $\mathbf{u}(t, \mathbf{u}_0)$ which starts at $\mathbf{u}_0 \in \mathbb{R}^3$. As we saw in Section 2, this solution exists for all time and converges to an equilibrium point $\mathbf{u}_\infty(\mathbf{u}_0) \in \mathbb{R}^3$.

We first derive a few general properties of solutions of Problem (3.1), and then focus on symmetric solutions, i.e. solutions in Π_2, in Section 3.1, on antisymmetric solutions in Section 3.2 and then on nonsymmetric solutions in Section 3.3.

We define the ellipse

$$S_\rho \stackrel{\text{def}}{=} \left\{(u_1, u_2, u_3) \in \mathbb{R}^3 : u_1^2 + u_1 u_3 + u_3^2 = \rho\right\}, \tag{3.2}$$

and we show:

Lemma 3.1 *Let $\mathbf{u}(t)$ be a solution of Problem (3.1). Then*

$$\begin{array}{lllll} \mathbf{u}(t) \to \Pi_2 & \textit{as} & t \to \infty & \textit{if} & 0 < \sigma \leqslant 2 \\ \mathbf{u}(t) \to \Pi_2 \cup S_\rho & \textit{as} & t \to \infty & \textit{if} & \sigma > 2, \end{array}$$

where $\rho = 1 - \frac{2}{\sigma}$.

Proof. We assume that $\mathbf{u}(t)$ is a nontrivial solution, and that $\mathbf{u}(t)$ tends to a limit $\mathbf{u}_\infty \neq 0$ as $t \to \infty$. Put

$$z \stackrel{\text{def}}{=} u_1 - u_3. \tag{3.3}$$

Then, subtracting the equation for u_3 from the one for u_1 we obtain

$$z' = \left\{-(2-\sigma) - \sigma\big(u_1^2 + u_1 u_3 + u_3^2\big)\right\} z. \tag{3.4}$$

Suppose that $z(0) > 0$. Then, equation (3.4) implies that $z(t) > 0$ for all $t \geqslant 0$. Since

$$u_1^2 + u_1 u_3 + u_3^2 = \tfrac{1}{2}(u_1 + u_3)^2 + \tfrac{1}{2}(u_1^2 + u_3^2) > 0,$$

because $\mathbf{u} \neq 0$, it then follows that

$$z' < -(2-\sigma) z,$$

and hence that

$$z(t) < z(0)\, e^{-(2-\sigma)t}. \tag{3.5}$$

Similarly, if $z(0) < 0$. Hence, if $\sigma \in [0, 2)$, then $z(t) \to 0$ as $t \to \infty$, and $\mathbf{u}(t) \to \Pi_2$.

Next, suppose that $\sigma = 2$. Then equation (3.4) becomes

$$z' = -2z\,(u_1^2 + u_1 u_3 + u_3^2).$$

Since we assume that $\mathbf{u}(t)$ tends to a nontrivial limit as $t \to \infty$, it follows that $u_1^2 + u_1 u_3 + u_3^2$ tends to a positive limit and hence we may conclude again that $|z(t)| \to 0$ exponentially.

Finally, suppose that $\sigma > 2$. Because $\mathbf{u}(t)$ tends to a nonzero limit as $t \to \infty$, it follows that the limit of the right hand side of (3.4) exists, and hence that $z'(t) \to 0$. This means that $\mathbf{u}_\infty \in S_\rho \cup \Pi_2$.

3.1 Symmetric solutions

When $u_1 = u_3$ the system (3.1) reduces to

$$\begin{cases} u_1' = -2u_1 + u_2 + \sigma f(u_1), & \text{(3.6a)} \\ u_2' = 2u_1 - 2u_2 + \sigma f(u_2). & \text{(3.6b)} \end{cases}$$

Before giving a complete characterisation of the equilibrium states, let us first give a brief description of the isoclines, which will help us to understand the structure. In Figure 2 we have plotted the different scenarios for different values of σ. When σ is close to zero we only have the trivial equilibrium state. Then, when σ is increased, two new equilibria bifurcate (supercritically) from the origin at $\sigma = 2 - \sqrt{2}$, one into the first quadrant, and one into the third quadrant of the (u_1, u_2)-plane. When σ exceeds the value 2, the slope of the isoclines at the origin becomes negative and at $\sigma = 2 + \sqrt{2}$ two new equilibrium states bifurcate (supercritically) from the origin, this time into the second and the fourth quadrant. Thus, on the branch emanating from the first bifurcation point u_1 and u_2 have the same sign, whilst on the branch emanating from the second bifurcation point u_1 and u_2 have opposite sign. Finally, at a value $\sigma > 2 + \sqrt{2}$ ($\hat{\sigma} \approx 6.85$) four new equilibria appear from saddle-node bifurcations. The value $\hat{\mu}$ is found to be the unique positive root of a sixth order polynomial.

$$4x^6 - 123x^4 + 768x^2 - 2048 = 0 \qquad (\hat{\mu} \approx 4.85).$$

In Figure 3, we show these results in a bifurcation diagram. We represent the stable equilibria with solid lines and the unstable ones with dashed lines.

In the next theorem we give the complete characterisation of the set of symmetric equilibrium solutions of Problem (3.6), as well as their stability properties.

Theorem 3.1 *The number of symmetric equilibria of equation* (2.1) *is given by:*

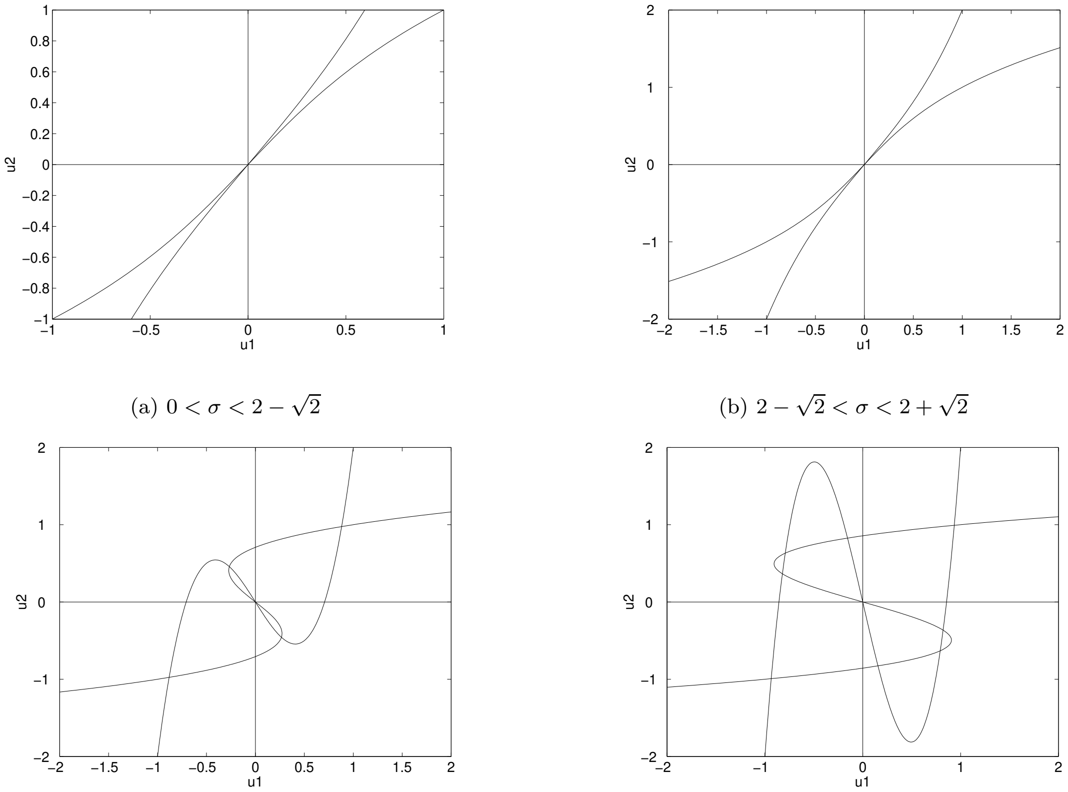

(a) $0 < \sigma < 2 - \sqrt{2}$

(b) $2 - \sqrt{2} < \sigma < 2 + \sqrt{2}$

(c) $2 + \sqrt{2} < \sigma < \hat{\sigma}$

(d) $\sigma > \hat{\sigma}$

Figure 2: Isoclines for different values of σ.

1. *If* $0 < \sigma < 2 - \sqrt{2}$*, then the origin is the unique equilibrium. It is stable.*

2. *If* $2 - \sqrt{2} < \sigma < 2 + \sqrt{2}$*, then there exist two nontrivial symmetric equilibria. They bifurcate from the origin at* $\sigma = 2 - \sqrt{2}$ *(supercritical pitchfork bifurcation) into the first and the third quadrant and they extend to* $\sigma =, \infty$*. They are stable nodes for every* $\sigma > 2 - \sqrt{2}$ *and in this regime, the origin is a saddle.*

3. *If* $2 + \sqrt{2} < \sigma < \hat{\sigma}$*, then there exist four nontrivial equilibrium states. The two new symmetric equilibria bifurcate from the origin at* $\sigma = 2 + \sqrt{2}$ *(supercritical pitchfork bifurcation) into the second and the fourth quadrant, and they extend to* $\sigma = \infty$*. They are saddles for every* $\sigma > 2 + \sqrt{2}$ *and the origin becomes an unstable node.*

4. *If* $\sigma > \hat{\sigma}$*, then there exist eight nontrivial equilibria. The four new sym-*

metric equilibria emerge at $\sigma = 2 + \hat{\mu}$ from a saddle-node bifurcation at a point in the second, respectively the fourth, quadrant. The equilibrium states with the highest value of $|u_2|$ are stable nodes and the other two are saddles.

The proof involves a detailed study of the phase plane, and of the two isoclines in particular. We give the details in the Appendix.

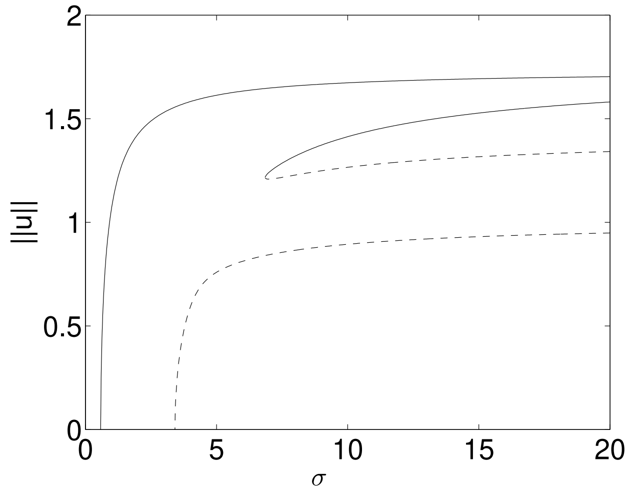

Figure 3: Bifurcation diagram of the symmetric equilibria

From Theorem 3.1 and inspection of the phase plane we can draw the following conclusions:

1. For $\sigma \leqslant 2-\sqrt{2}$ the trivial solution $\mathbf{u}=0$ is stable and for all $\sigma > 2-\sqrt{2}$ it is unstable.

2. For any $\sigma > 2-\sqrt{2}$ there exists a unique symmetric equilibrium state $\mathbf{u}^*$ in the first quadrant and its domain of attraction includes the first quadrant. Similarly, $-\mathbf{u}^*$ is the unique symmetric equilibrium state in the third quadrant, attracting all symmetric orbits that start in this quadrant as $t \to \infty$.

   For symmetric solutions the action $J_F(\mathbf{u})$ defined in (2.5) is given by

$$J_F(\mathbf{u}) = u_1^2 + (u_2 - u_1)^2 - \frac{\sigma}{2}(2u_1^2 + u_2^2) + \frac{\sigma}{4}(2u_1^4 + u_2^4). \tag{3.7}$$

3. For $\sigma \leqslant 2-\sqrt{2}$ the trivial solution is the global minimiser of $J_F(\mathbf{u})$, and for $\sigma > 2-\sqrt{2}$ the global minimiser is nontrivial.

Since J_F decreases along orbits, it follows from the second observation that J_F attains its minimum value in the first quadrant at $\mathbf{u}^*$. In the following theorem we show that

$$J_F(\mathbf{u}^*) = \min\{J_F(\mathbf{y}) : \mathbf{y} \in \mathbb{R}^2\}.$$

Theorem 3.2 *Let $\sigma > 2 - \sqrt{2}$. Then $\mathbf{u}^*$ and $-\mathbf{u}^*$ are the global minimisers of J_F in $\mathbb{R}^2$.*

Proof. We have seen in Theorem 3.1 that because $\mathbf{u}^*$ attracts all the orbits that start in the first quadrant, it is the global minimiser of J_F in this quadrant. Suppose that J_F has a local minimum at a point $\mathbf{y}^*$ in the interior of the fourth quadrant. Write

$$u_1 = y_1 \qquad \text{and} \qquad u_2 = -y_2.$$

Then the point $\mathbf{u} = (u_1, u_2)$ lies in the first quadrant. Moreover, we see from (3.7) that

$$\begin{aligned} J_F(\mathbf{u}) &= y_1^2 + (y_2 + y_1)^2 - \frac{\sigma}{2}(2y_1^2 + y_2^2) + \frac{\sigma}{4}(2y_1^4 + y_2^4) \\ &= J_F(\mathbf{y}) + (y_2 + y_1)^2 - (y_2 - y_1)^2 \\ &= J_F(\mathbf{y}) + 4y_1 y_2 < J_F(\mathbf{y}). \end{aligned}$$

Since $J_F(\mathbf{u}) \geqslant J_F(\mathbf{u}^*)$ for all $\mathbf{u}$ in the first quadrant, it follows that $J_F(\mathbf{y}) > J_F(\mathbf{u}^*)$, so that $\mathbf{y}$ cannot be a global minimiser in $\mathbb{R}^2$.

So far these properties all mirror properties of the Fisher-Kolmogorov equation. The next property, however, introduces a difference between the discrete and the continuous problem.

4. For every $\sigma > \hat{\sigma}$, there exist *stable* states ξ and $-\xi$ in the second, respectively the fourth quadrant. Therefore, there exist initial data which yield orbits that converge to a final state which does not have one sign.

In conclusion we note that the problem discussed in this subsection has much in common with linear diffusion in a slab under the influence of nonlinear boundary conditions, as was discussed by Aris [1] and Aronson & Peletier [2].

3.2 Antisymmetric solutions

When $u_3 = -u_1$ and $u_2 = 0$ the system (3.1) reduces to

$$u_1' = (\sigma - 2)\, u_1 - \sigma u_1^3. \tag{3.8}$$

We will call equation (3.8) the *reduced antisymmetric system*. The following Theorem gives us the main result about existence and stability of nontrivial antisymmetric solutions. Recall that nontrivial antisymmetric points are of the form $\mathbf{u} = k(1\ 0\ -1)$ for some $k \in \mathbb{R},\ k \neq 0$.

Theorem 3.3 *Let $\mathbf{u}(t)$ be a nontrivial antisymmetric solution.*

1. *If $\sigma \leqslant 2$, then*
$$\mathbf{u}(t) \to 0, \qquad \textit{as} \quad t \to \infty.$$

2. *If $\sigma > 2$, then*
$$\mathbf{u}(t) \to \pm\sqrt{1-\frac{2}{\sigma}}\,(1\ 0\ -1)\,, \qquad \textit{as} \quad t \to \infty,$$
where $\mathrm{sgn}\,(u_1(t)) = \mathrm{sgn}(k)$.

With respect to the system (3.1)*, the nontrivial antisymmetric equilibria* $\pm\mathbf{u}(\sigma)$ *are locally unstable for every* $\sigma > 2$.

Proof. Existence of nontrivial antisymmetric equilibria follows directly from equation (3.8). When $\sigma \leqslant 2$, the antisymmetric solution converges to the origin and for $\sigma > 2$, the origin loses stability and the bifurcating nontrivial antisymmetric equilibria are stable. As equation (3.8) is one dimensional, the final profile is determined by the sign of $u_1(0)$.

Let us study the question of stability of the nontrivial equilibria for $\sigma > 2$ in the system (3.1). We linearise the system around the nontrivial antisymmetric equilibrium. The stability matrix is given by
$$\begin{pmatrix} 4-2\sigma & 1 & 0 \\ 1 & \sigma-2 & 1 \\ 0 & 1 & 4-2\sigma \end{pmatrix}.$$
and its eigenvalues are the following:
$$\begin{aligned} \lambda_1(\sigma) &= 4-2\sigma < 0, \\ \lambda_2(\sigma) &= 1-\frac{\sigma}{2}-\frac{\sqrt{9\sigma^2-36\sigma+44}}{2} < 0, \\ \lambda_3(\sigma) &= 1-\frac{\sigma}{2}+\frac{\sqrt{9\sigma^2-36\sigma+44}}{2} > 0, \end{aligned}$$
so that the equilibrium is unstable.

3.3 Nonsymmetric equilibria

Since by Lemma 3.2, any solution of the full system tends to Π_2 as $t \to \infty$ if $\sigma \leqslant 2$, we have the following nonexistence theorem.

Theorem 3.4 *For $\sigma \leqslant 2$ there exist no nonsymmetric equilibrium states.*

The result of this theorem is optimal because for every $\sigma > 2$ we have two *antisymmetric* equilibrium states bifurcating from the trivial solution at $\sigma = 2$, found in the previous subsection.

The result of a numerical search for more nonsymmetric equilibria is summarized in the following proposition, and the bifurcation picture is shown in Figure 4, where we plot $\|u\|$ vs. σ.

Proposition 3.1 *For $\sigma \in (0,2]$, every equilibrium is symmetric. For $\sigma \in (2, 2+2\sqrt{2})$, every equilibrium is either symmetric or antisymmetric. For $\sigma \geqslant 2+2\sqrt{2}$, there exist 16 new nonsymmetric equilibrium states. They all emerge from saddle-node bifurcations at $\sigma = 2+2\sqrt{2}$.*

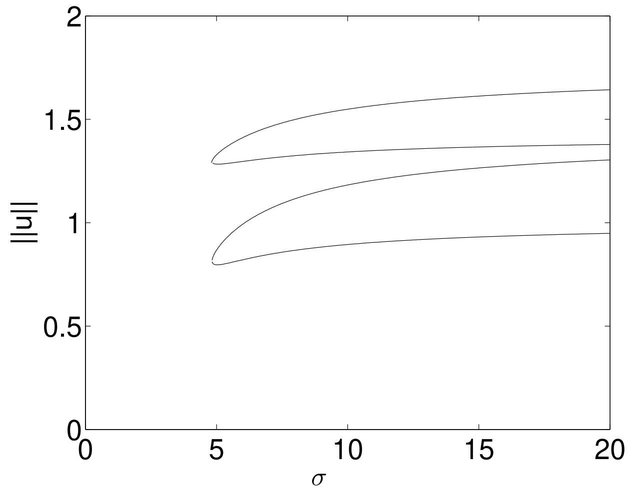

Figure 4: Bifurcation diagram of the nonsymmetric equilibrium states

Note that if $\mathbf{u}$ is a nonsymmetric equilibrium state, then so are $-\mathbf{u}$ and $\pm L_2(\mathbf{u})$, where L_2 denotes the operator that reflects $\mathbf{u}$ with respect to the central node u_2. Thus, the 16 new nonsymmetric solutions consist of 4 different branches of solutions.

4 The discrete Swift-Hohenberg equation

Here we turn to the discrete Swift-Hohenberg equation on a lattice of 5 nodes, $u_0, \ldots, u_4$. At the end points of the lattice we impose the conditions

$$u_0 = 0, \qquad u_4 = 0 \qquad \text{and} \qquad u_{-1} = -u_1, \qquad u_5 = -u_3,$$

where the virtual nodes u_{-1} and u_5 need to be introduced to make the equation for the points u_1, u_2 and u_3 well defined. We then obtain the following system

$$\begin{cases} u_1' = (-5\gamma^2 + 4\gamma)u_1 + (4\gamma^2 - 2\gamma)u_2 - \gamma^2 u_3 - f_\alpha(u_1), \\ u_2' = (4\gamma^2 - 2\gamma)u_1 + (-6\gamma^2 + 4\gamma)u_2 + (4\gamma^2 - 2\gamma)u_3 - f_\alpha(u_2), \\ u_3' = -\gamma^2 u_1 + (4\gamma^2 - 2\gamma)u_2 + (-5\gamma^2 + 4\gamma)u_3 - f_\alpha(u_3), \end{cases} \tag{4.1}$$

where

$$f_\alpha(s) = (1-\alpha)s + s^3.$$

As with the discrete Fisher-Kolmogorov equation, for α sufficiently small, orbits of Problem (4.1) eventually approach a symmetric state, i.e. they tend to the plane Π_2. Specifically we have:

Lemma 4.1 *Let $\mathbf{u}(t)$ be a solution of Problem (4.1). Then*

$$\begin{array}{llll} \mathbf{u}(t) \to \Pi_2 & \textit{as} \quad t \to \infty & \textit{if} & 0 < \alpha \leqslant (2\gamma - 1)^2, \\ \mathbf{u}(t) \to \Pi_2 \cup S_\delta & \textit{as} \quad t \to \infty & \textit{if} & \alpha > (2\gamma - 1)^2, \end{array}$$

where $\delta = \alpha - (2\gamma - 1)^2$.

The proof is similar to that of Lemma 3.1, and we omit it here.

In order to determine the linear stability of $\mathbf{u} = 0$, we substitute $\mathbf{u}(t) = e^{-\lambda t}\mathbf{e}$ into the system (4.1) and omit higher order terms. This leads to an eigenvalue problem with eigenvectors

$$\mathbf{e}_1 = (1, \sqrt{2}, 1)^T, \qquad \mathbf{e}_2 = (1, 0, -1)^T, \qquad \mathbf{e}_3 = (1, -\sqrt{2}, 1)^T. \tag{4.2}$$

with corresponding eigenvalues

$$\lambda_1 = -p - q\sqrt{2}, \qquad \lambda_2 = (2\gamma - 1)^2 - \alpha, \qquad \lambda_3 = -p + q\sqrt{2}, \tag{4.3}$$

where

$$p(\alpha, \gamma) \stackrel{\text{def}}{=} -6\gamma^2 + 4\gamma - 1 + \alpha, \qquad q(\gamma) \stackrel{\text{def}}{=} 4\gamma^2 - 2\gamma. \tag{4.4}$$

Note that we can write λ_1 and λ_3 as

$$\lambda_1 = \{(2 - \sqrt{2})\gamma - 1\}^2 - \alpha \qquad \text{and} \qquad \lambda_3 = \{(2 + \sqrt{2})\gamma - 1\}^2 - \alpha, \tag{4.5}$$

Plainly, $\mathbf{e}_1$ and $\mathbf{e}_3$ together span the set of symmetric solutions, whilst $\mathbf{e}_2$ spans the set of anti-symmetric solutions. In fact, writing $\mathbf{u}(t) = \phi(t)\mathbf{e}_2$, we find the following equation for $\phi(t)$:

$$\phi' = \{\alpha - (2\gamma - 1)^2\}\phi - \phi^3. \tag{4.6}$$

which yields the following result:

Theorem 4.1 *Let $\delta = \alpha - (2\gamma - 1)^2$, and let $\mathbf{u}(t)$ be a nontrivial antisymmetric solution such that $\mathbf{u}(0) = k\mathbf{e}_2$ for some $k \in \mathbb{R}$.*

(a) *If $\delta \leqslant 0$, then*

$$\mathbf{u}(t) \to 0 \qquad \textit{as} \qquad t \to \infty.$$

(b) *If $\delta > 0$, then*

$$\mathbf{u}(t) \to \sqrt{\delta} \cdot \operatorname{sgn}(k)\, \mathbf{e_2} \qquad \textit{as} \qquad t \to \infty.$$

4.1 Symmetric dynamics

For symmetric solutions we have $u_1 = u_3$, so that the system (4.1) reduces to

$$\begin{cases} u_1' = (-6\gamma^2 + 4\gamma)u_1 + (4\gamma^2 - 2\gamma)u_2 - (1-\alpha)u_1 - u_1^3, \\ u_2' = (8\gamma^2 - 4\gamma)u_1 + (-6\gamma^2 + 4\gamma)u_2 - (1-\alpha)u_2 - u_2^3, \end{cases} \tag{4.7}$$

or, written more compactly,

$$\begin{cases} u_1' = pu_1 + qu_2 - u_1^3, \\ u_2' = 2qu_1 + pu_2 - u_2^3. \end{cases} \tag{4.8}$$

The two equations are coupled through the term involving the coefficient q. Hence, if $q = 0$, which is the case when $\gamma = \frac{1}{2}$, the system uncouples and we obtain two identical equations for u_1 and u_2:

$$\begin{cases} u_1' = \left(\alpha - \dfrac{1}{2}\right) u_1 - u_1^3, \\ u_2' = \left(\alpha - \dfrac{1}{2}\right) u_2 - u_2^3. \end{cases} \tag{4.9}$$

We see that if $\alpha < \frac{1}{2}$, then the origin is stable, and all orbits converge to it, and if $\alpha > \frac{1}{2}$ it is unstable, and we have 8 nontrivial equilibrium states:

$$(\pm\rho, 0), \qquad (0, \pm\rho), \qquad \text{and} \qquad (\pm\rho, \pm\rho),$$

where $\rho = \sqrt{\alpha - \frac{1}{2}}$. The ones on the axes are unstable; the other ones are stable.

The linear stability of the trivial solution $\mathbf{u} = 0$ depends on the sign of the eigenvalues λ_1 and λ_3. If they are both positive the origin is stable; if one is negative it is unstable. It follows from (4.8) that

$$\lambda_1 < 0 \qquad \text{if} \qquad \gamma \in I_1 \stackrel{\text{def}}{=} (\gamma_1^-, \gamma_1^+),$$

where

$$\gamma_1^{\pm}(\alpha) = \left(1 + \frac{\sqrt{2}}{2}\right)\left(1 \pm \sqrt{\alpha}\right). \tag{4.10}$$

Similarly, we find that

$$\lambda_3 < 0 \qquad \text{if} \qquad \gamma \in I_3 \stackrel{\text{def}}{=} (\gamma_3^-, \gamma_3^+),$$

where

$$\gamma_3^{\pm}(\alpha) = \left(1 - \frac{\sqrt{2}}{2}\right)\left(1 \pm \sqrt{\alpha}\right). \tag{4.11}$$

Note that if $\alpha < \frac{1}{2}$ then the intervals $I_1(\alpha)$ and $I_3(\alpha)$ are disjoint, that

$$\gamma_1^+(\alpha) \to \frac{1}{2} \qquad \text{and} \qquad \gamma_3^-(\alpha) \to \frac{1}{2} \qquad \text{as} \qquad \alpha \to \frac{1}{2},$$

and that they overlap if $\alpha \in (\frac{1}{2}, 1)$.

When I_1 and I_3 are disjoint, the situation is relatively simple, and we discuss this case first.

The case $0 < \alpha < \frac{1}{2}$

As in Section 3 we first give an overview of the situation by following the isoclines in the phase plane as γ decreases. Remembering that γ was introduced as L^{-2}, this corresponds to the length L of the interval increasing and, as expected from the continuous problem, the complexity of the solution set, and the solution graphs, increases as well. In Figure 5 the phase plane is shown at four different values of γ when $\alpha = 0.3$.

We see that for $\gamma > \gamma_1^+$ the isoclines only intersect at the origin, so that the origin is the unique equilibrium state. It is clearly a global attractor. However, γ drops below γ_1^+ two nontrivial solutions $\pm\mathbf{u}_1(\gamma)$ bifurcate from the origin, one into the first quadrant, and one into the third. They continue to exist until γ reaches γ_1^-, when they merge with the trivial solution again. For $\gamma \in [\gamma_3^+, \gamma_1^-]$ the origin remains the only equilibrium state, but at γ_3^+ two nontrivial solutions $\mathbf{u}_3(\gamma)$ bifurcate again from the origin, this time into the second and the fourth quadrant. They too, return to the trivial solution, at γ_3^-. For γ below γ_3^- the trivial solution is the unique equilibrium state. The situation is illustrated in a bifurcation diagram in Figure 6. These results are summarised in the following theorem, in which

$$I_1(\alpha) = \left(\gamma_1^-(\alpha), \gamma_1^+(\alpha)\right) \qquad \text{and} \qquad I_3(\alpha) = \left(\gamma_3^-(\alpha), \gamma_3^+(\alpha)\right).$$

Theorem 4.2 *Suppose that* $0 < \alpha < \frac{1}{2}$.

(a) If $\gamma \in \mathbb{R}^+ \setminus (I_1 \cup I_3)$, then the origin is the unique equilibrium state, and it attracts all orbits.

(b) If $\gamma \in I_1$, then there exist two equilibrium states $\pm\mathbf{u}_1(\gamma)$, one in the first quadrant, and one in the third. The origin is now unstable and $\pm\mathbf{u}_1$ are stable.

(c) If $\gamma \in I_3$, then there exist two equilibrium states $\pm\mathbf{u}_3(\gamma)$, one in the second quadrant, and one in the fourth. The origin is unstable and $\pm\mathbf{u}_3$ are also unstable.

The proof of this theorem is similar to that of Theorem 3.1, and we omit it.

In Figure 6, we fix $\alpha = 0.3$ and we plot the norm $\|\mathbf{u}(\gamma)\|$ versus γ, where

$$\|\mathbf{u}\| = \sqrt{2u_1^2 + u_2^2},$$

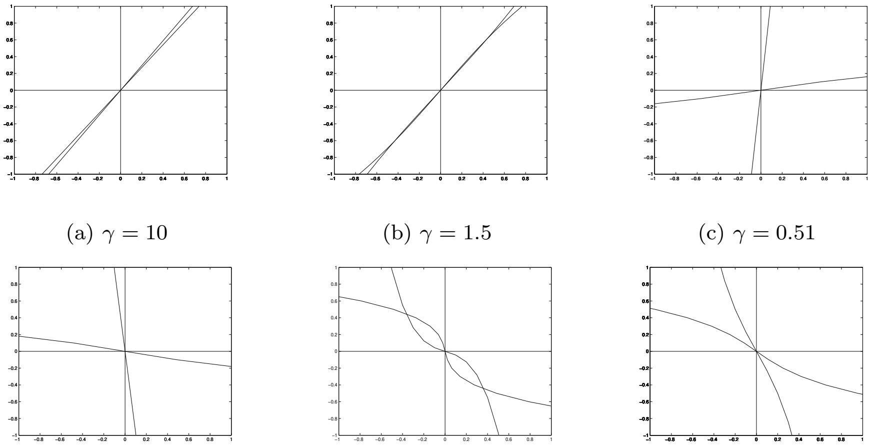

(a) $\gamma = 10$ (b) $\gamma = 1.5$ (c) $\gamma = 0.51$

(d) $\gamma = 0.49$ (e) $\gamma = 0.4$ (f) $\gamma = 0.1$

Figure 5: Isoclines for $\alpha = 0.3$ and different values of γ.

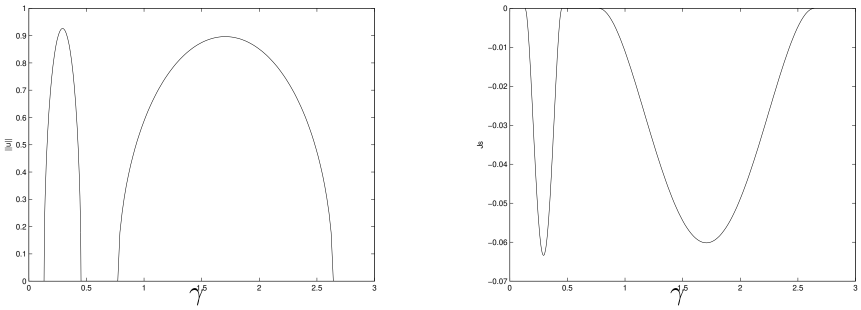

(a) $\|\mathbf{u}\|$ vs. γ. (b) J_s vs. γ.

Figure 6: Graph of $\|\mathbf{u}\|$ and J_s versus γ for $\alpha = 0.3$

and the action J of all the equilibria versus γ. We can easily identify the intervals I_1 and I_3 as those where there exist nontrivial symmetric stable equilibria and the action J is negative.

The case $\frac{1}{2} < \alpha < 1$

In this regime of α the intervals I_1 and I_3 overlap, and the structure of the solution set is much more complicated. In Figures 7 and 8 we show bifurcation pictures for $\alpha = 0.7$. In Figure 7 we have put the norm $\|\mathbf{u}\|$ along the vertical axis. We represent stable equilibria with solid line and unstable equilibria with dashed line. In Figure 8, we have put u_1 and u_2 along the vertical axis. Since the situation near $\gamma = \frac{1}{2}$ is rather complex, we also present a blow up of the graph for u_1 near $\gamma = \frac{1}{2}$.

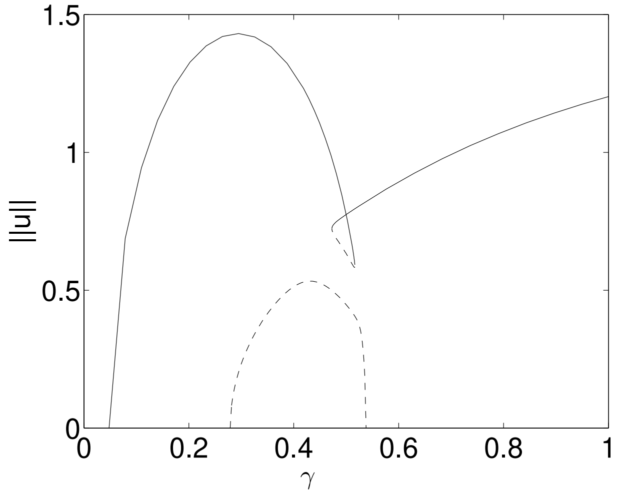

Figure 7: Graph of $\|\mathbf{u}\|$ versus γ for $\alpha = 0.7$

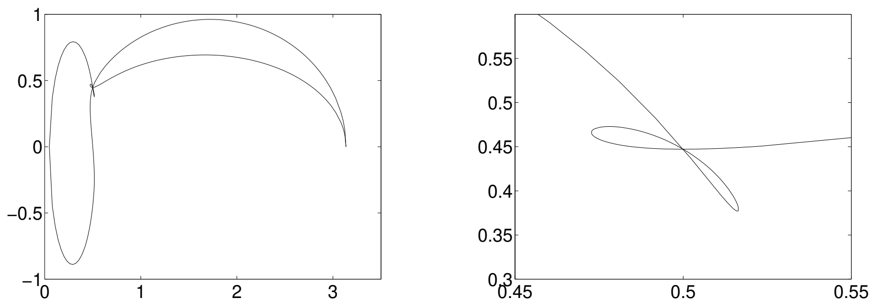

(a) u_1 and u_2 vs. γ.

(b) u_1 vs. γ, amplified.

Figure 8: Graph of u_1 and u_2 versus γ for $\alpha = 0.7$

Again, we first inspect the evolution of the isoclines in the phase plane when γ varies from large to small values. The first sequence of phase portraits is shown in Figure 9. We see that as γ passes γ_1^+, then as in the previous case, two equilibrium solutions bifurcate from the trivial solution, one into the first quadrant, and one into the third. We denote them again by $\pm\mathbf{u}$. Then, still as before, at γ_3^+ a second pair of equilibrium states, $\pm\mathbf{y}$ bifurcate from the trivial solution, one into the second quadrant, and one into the fourth. Reducing γ further, we encounter a saddle-node bifurcation at $\gamma = \gamma_*^+$, which creates two new equilibrium states $\mathbf{z}^*$ and $\mathbf{z}^{**}$ in the second quadrant, and $-\mathbf{z}^*$ and $-\mathbf{z}^{**}$ in the fourth quadrant.

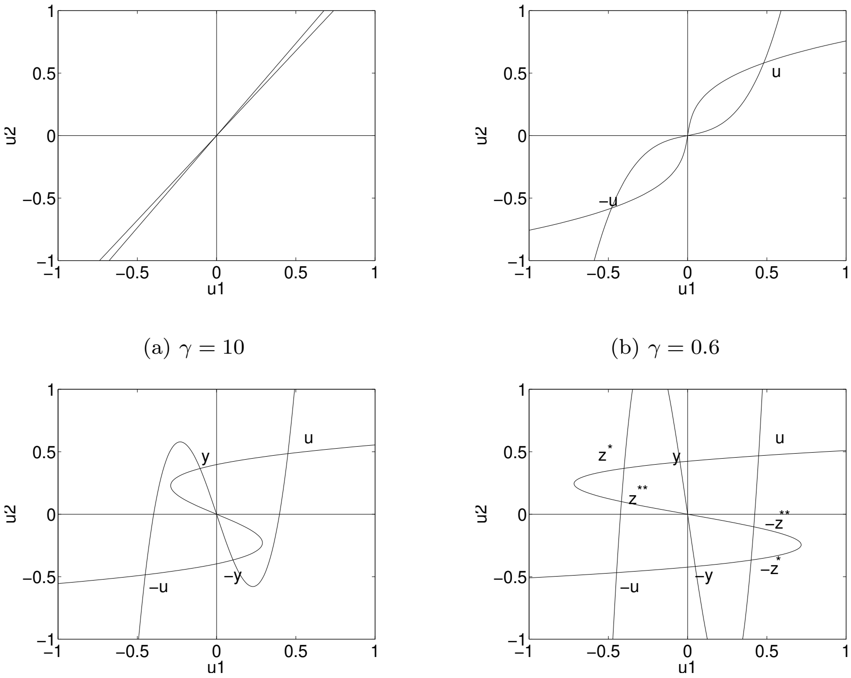

(a) $\gamma = 10$

(b) $\gamma = 0.6$

(c) $\gamma = 0.52$

(d) $\gamma = 0.51$

Figure 9: Isoclines for $\alpha = 0.7$ and different values of γ.

When we approach $\gamma = \frac{1}{2}$ we have

$$\mathbf{u} \to (\rho, \rho), \qquad \mathbf{y} \to (0, \rho), \qquad \mathbf{z}^* \to (\rho, -\rho), \qquad \mathbf{z}^{**} \to (\rho, 0),$$

where $\rho = \sqrt{\alpha - \frac{1}{2}}$. This is shown in Figure 10. Note that the axes are isoclines for $\gamma = \frac{1}{2}$.

For $\gamma < \frac{1}{2}$, the eight nontrivial equilibria gradually disappear by bifurcation phenomena similar to the way they emerged. The first bifurcation is of saddle-node type at $\gamma = \gamma_*^-$, and the disappearing equilibria are $\pm\mathbf{u}$ and $\pm\mathbf{z}^{**}$. As γ passes through γ_1^-, the equilibria $\pm\mathbf{y}$ disappear by a bifurcation to the origin. Finally, reducing γ further, as γ passes through γ_3^-, the equilibria $\pm\mathbf{z}^*$ disappear, again by a bifurcation to the origin. For $\gamma < \gamma_3^-$, the origin is the unique

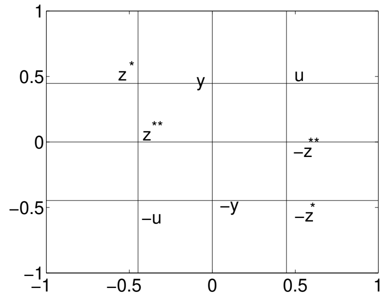

Figure 10: Isoclines for $\alpha = 0.7$ and $\gamma = 0.5$.

equilibrium. This sequence of events is illustrated in the four plots of Figure 11 and summarised in the following theorem.

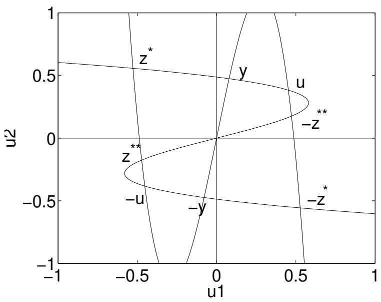

(a) $\gamma = 0.48$

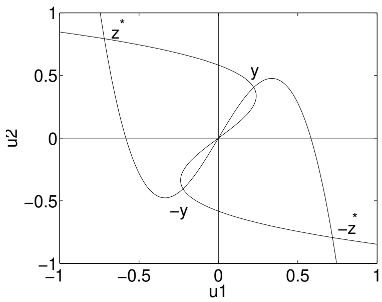

(b) $\gamma = 0.4$

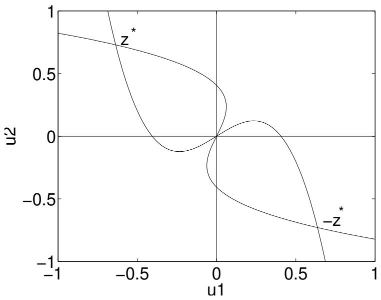

(c) $\gamma = 0.15$

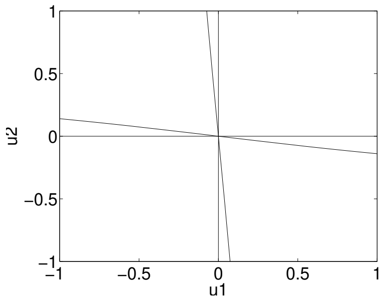

(d) $\gamma = 0.01$

Figure 11: Isoclines for $\alpha = 0.7$ and different values of γ.

Theorem 4.3 *Suppose that $\frac{1}{2} < \alpha < 1$. Then, there exist*

$$\gamma_3^-(\alpha) < \gamma_1^-(\alpha) < \gamma_*^-(\alpha) < \frac{1}{2} < \gamma_*^+(\alpha) < \gamma_3^+(\alpha) < \gamma_1^+(\alpha),$$

such that:

(a) If $\gamma \in \mathbb{R}^+ \setminus (\gamma_3^-, \gamma_1^+)$, the origin is the unique equilibrium state and it attracts all orbits.

(b) If $\gamma_*^- < \gamma < \gamma_1^+$, a pair of nontrivial equilibria $\pm\mathbf{u}$ exist, one in the first quadrant and one in the third. At $\gamma = \gamma_*^-$, $\mathbf{u}$ has a saddle-node bifurcation and at γ_1^+, it has a supercritical bifurcation from the origin. $\mathbf{u}$ is a stable equilibrium and it is the minimizer for $\frac{1}{2} < \gamma < \gamma_1^+$.

(c) If $\gamma_1^- < \gamma < \gamma_3^+$, a pair of nontrivial equilibria $\pm\mathbf{y}$ exist. For $\gamma_1^- < \gamma < \frac{1}{2}$, they are located in the second quadrant (respectively the fourth) and for $\frac{1}{2} < \gamma < \gamma_3^+$, they are located in the first quadrant (respectively, the third). They are all saddles.

(d) If $\gamma_3^- < \gamma < \gamma_*^+$, a pair of nontrivial equilibria $\pm\mathbf{z}^*$ exist, one in the second quadrant and one in the fourth. At $\gamma = \gamma_*^+$, it has a saddle-node bifurcation and at $\gamma = \gamma_3^-$ it has a supercritical bifurcation from the origin. $\pm\mathbf{z}^*$ are stable and they are minimizers for $\gamma_3^- < \gamma < \frac{1}{2}$.

(e) If $\gamma_*^- < \gamma < \gamma_*^+$, a pair of nontrivial equilibria $\pm\mathbf{z}^{**}$ exist. For $\gamma_1^- < \gamma < \frac{1}{2}$, they are located in the second quadrant (respectively the fourth) and for $\frac{1}{2} < \gamma < \gamma_3^+$, they are located in the third quadrant (respectively, the first). They are saddles.

The proof of this theorem is obtained analytically in a similar way as the proof of Theorem 3.1 and we omit it here.

Next, we want to describe the bifurcation diagram of equilibria shown in Figure 8. A simple bifurcation theorem shows that around the critical values $\gamma_1^-, \gamma_1^+, \gamma_3^-, \gamma_3^+$ there exist local bifurcation branches. These branches can be continued as long as the conditions for the Implicit Function Theorem hold, that is, as long as the appropriate determinant does not vanish. Applying this argument to this case, we find by a combination of analytical and numerical arguments that one branch can be extended smoothly along the interval $[\gamma_1^-, \gamma_3^+]$, and the other one can be extended continuously but not smoothly along $[\gamma_3^-, \gamma_1^+]$. The reason for the lack of smoothness is that the corresponding determinant mentioned above vanishes. This occurs precisely at γ_*^- and γ_*^+: they are the values of γ for which both isoclines touch tangentially. This is summarised in the following proposition:

Proposition 4.1 *There exists an smooth parametrization $h_1 : [0,1] \to [\gamma_1^-, \gamma_3^+] \times \mathbb{R}^3$ with components $s \to (\gamma, u_1, u_2, u_3)$ and a continuous (but not smooth) parametrization $h_2 : [0,1] \to [\gamma_3^-, \gamma_1^+] \times \mathbb{R}^3$ such that* *(a)* $h_1(0) = (\gamma_1^-, 0, 0, 0)$, $h_1(1) = (\gamma_3^+, 0, 0, 0)$, *and* $\frac{\partial\gamma}{\partial s}$ *is continuous and positive on* $s \in (0, 1)$.

(b) $h_2(0) = (\gamma_3^-, 0, 0, 0)$, $h_2(1) = (\gamma_1^+, 0, 0, 0)$, *and* $\frac{\partial\gamma}{\partial s}$ *is discontinuous on* $s \in (0, 1)$. *The discontinuity of* $\frac{\partial\gamma}{\partial s}$ *occurs at* $\gamma = \gamma_*^-$ *and* $\gamma == \gamma_*^+$.

(c) $h_1(\cdot)$ *and* $h_2(\cdot)$ *represent all the symmetric equilibria of the discrete SH equation, up to symmetry. More specifically, let* $(\gamma, \mathbf{u})$ *be a nontrivial symmetric equilibrium of the discrete SH equation. Then, there exists a unique* $s \in (0, 1)$ *and a unique* $i \in \{1, 2\}$ *such that either* $h_i(s) = (\gamma, \mathbf{u})$ *or* $h_i(s) = (\gamma, -\mathbf{u})$.

The local results of this proposition can be proved analytically, by a simple bifurcation argument. When the local results are obtained, then the Implicit Function Theorem states that the local result can be extended to an interval where the appropriate determinant of the Jacobian matrix does not vanish. This condition is checked numerically.

5 Dynamics

In the previous section we have obtained a complete description of the set equilibrium solutions of the discrete Swift-Hohenberg equation for different values of α and γ. Knowing that solutions of the discrete Swift-Hohenberg equation converge to one of these equilibrium solutions, we will ask in this section which particular equilibrium solution will be selected. In [7] and [8] this same question was discussed for the Swift-Hohenberg equation. The phenomena observed there were in part a motivation for the study presented in this paper.

Throughout this section we shall assume that the initial value $\mathbf{u}_0$ is symmetric, and hence the solution $\mathbf{u}(t)$ will be symmetric for all time. Thus, we shall be studying solutions of the system (4.7):

$$\left\{ \begin{array}{rcl} u_1' & = & (-6\gamma^2 + 4\gamma)u_1 + (4\gamma^2 - 2\gamma)u_2 - (1-\alpha)u_1 - u_1^3, \\ u_2' & = & (8\gamma^2 - 4\gamma)u_1 + (-6\gamma^2 + 4\gamma)u_2 - (1-\alpha)u_2 - u_2^3. \end{array} \right. \tag{5.1}$$

If $0 < \alpha < \frac{1}{2}$, then for any given $\gamma > 0$, the set of equilibrium solutions is very limited. It consists of the origin and, for some values of γ, of a pair of nontrivial solutions.

If $\frac{1}{2} < \alpha < 1$, then, depending on the value of γ, there are many more nontrivial equilibrium solutions. Therefore, here we shall focus on this case. First, let us exhibit the critical values found in the previous section for $\alpha = 0.7$:

$$\begin{array}{lll} \gamma_3^- \approx 0.04784, & \gamma_1^- \approx 0.27884, & \gamma_*^- \approx 0.47272, \\ \gamma_*^+ \approx 0.51651, & \gamma_3^+ \approx 0.53795, & \gamma_1^+ \approx 3.13537. \end{array} \tag{5.2}$$

As in [7] and [8], we begin with a series of numerical experiments, and follow orbits for different values of γ. We shall firstdo this for

$$\mathbf{u}_0 = \left(\sin\left(\frac{\pi}{4}\right), \sin\left(\frac{\pi}{2}\right)\right) = \left(\frac{1}{\sqrt{2}}, 1\right) \qquad \text{and} \qquad \alpha = 0.7. \tag{5.3}$$

In [7] and [8] the large time behaviour of solutions was studied for increasing values of L. Thus, to emulate this analysis we consider a decreasing sequence of values of $\gamma = 1/L^2$. In Figure 12 we show solution profiles corresponding to six values of γ: $\gamma = 4,\ 3,\ 0.48,\ 0.47,\ 0.05$ and 0.01. Given the initial condition $\mathbf{u}_0$, we will denote the orbit by $\phi_t(\mathbf{u}_0, \gamma)$ and the final equilibrium by $\phi_\infty(\mathbf{u}_0, \gamma)$. We plot the initial profile $\mathbf{u}_0$ by a solid line, a few intermediate profiles by dashed lines and the final profile $\phi_\infty(\mathbf{u}_0, \gamma)$ by a thick line.

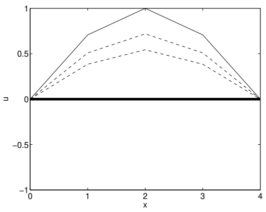

(a) $\gamma = 4$

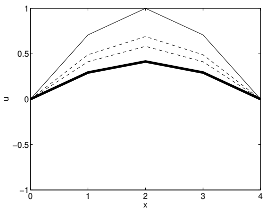

(b) $\gamma = 3$

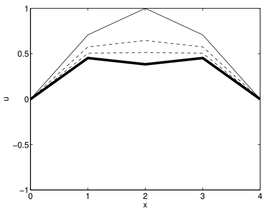

(c) $\gamma = 0.48$

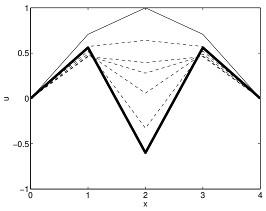

(d) $\gamma = 0.47$

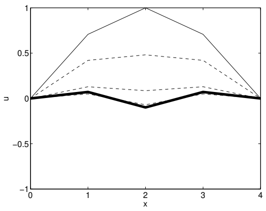

(e) $\gamma = 0.05$

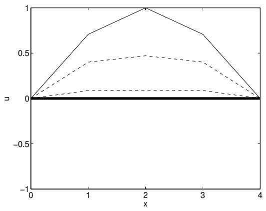

(f) $\gamma = 0.01$

Figure 12: Dynamics for $\alpha = 0.7$ and different values of γ.

It is evident that the final profile $\phi_\infty(\mathbf{u}_0, \gamma)$ depends critically on the value of γ. In order to follow the change in $\phi_\infty(\mathbf{u}_0, \gamma)$ more accurately as γ changes, we show in Figure 13 the action $J\big(\phi_\infty(\mathbf{u}_0, \gamma)\big)$ as γ varies, again for the choice of $\mathbf{u}_0$ and α given in (5.3).

We see that for $\gamma = 4$ the orbit converges to the origin. Indeed, since $\gamma_1^+ = 3.135...$ for $\alpha = 0.7$, we know that for $\gamma = 4$ the origin is the only equilibrium state. We see that when $\gamma = 3$, and hence has dropped below γ_1^+, the final state is no longer the trivial solution, but the unique solution (v_1, v_2), which lies in the first quadrant, and on the branch of solutions which bifurcates

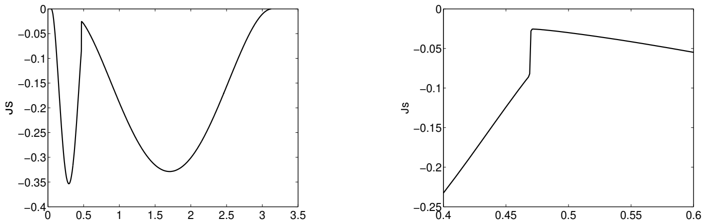

(a) $J_s\big(\phi_\infty(\mathbf{u}_0,\gamma)\big)$ vs. γ

(b) $J_s\big(\phi_\infty(\mathbf{u}_0,\gamma)\big)$ vs. γ, amplified

Figure 13: $J_s\big(\phi_\infty(\mathbf{u}_0,\gamma)\big)$ vs. γ for the choice (5.3)

subcritically from the trivial solution at γ_1^+. This equilibrium was denoted in the previous section by $\mathbf{u}$. As γ is reduced further, we see that around $\gamma = 0.47$, the graph of $J\big(\phi_\infty(\mathbf{u}_0,\gamma)\big)$ exhibits a discontinuity, and that $\phi_\infty(\mathbf{u}_0,\gamma)$ jumps from a profile in the first quadrant at $\gamma = 0.48$ to one which lies in the fourth quadrant at $\gamma = 0.47$. This equilibrium was denoted in the previous section by $-\mathbf{z}^*$. As γ is reduced further, $\phi_\infty(\mathbf{u}_0,\gamma)$ remains in the fourth quadrant and becomes the trivial solution again at $\gamma = \gamma_3^-$. In Figure 14 we can clearly view the jump of the final profile $\phi_\infty(\mathbf{u}_0,\gamma)$. There we draw in the phase plane the isoclines (in solid line) and the orbits (in thick line) followed by solution of equation (5.1) for the choice for α and $\mathbf{u}_0$ given by (5.3) and two different values of the parameter γ : 0.47 and 0.48.

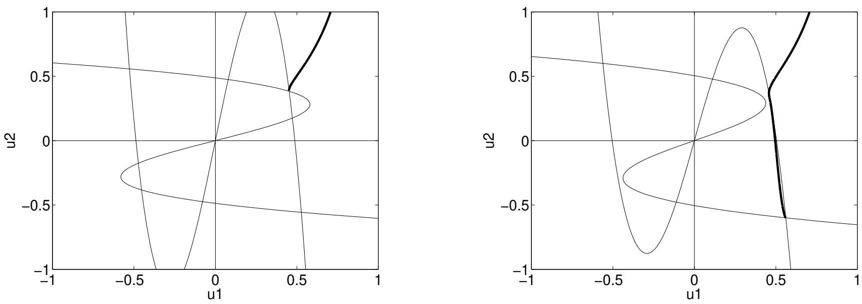

(a) $\gamma = 0.48$.

(b) $\gamma = 0.47$.

Figure 14: Graphs of the isoclines and orbits for symmetric discrete SH equation and conditions given by (5.3)

We will introduce some technical definitions that are motivated by our numerical simulations in order to describe the dynamics and, mor specifically, the variation of $\phi_\infty(\mathbf{u}_0, \gamma)$ with respect to γ and $\mathbf{u}_0$. In the next section, we will make phase plane analysis. It will shed some light and help us to understand the previous simulations.

As we have seen, the final profile $\phi_\infty(\mathbf{u}_0, \gamma)$ varies with γ. Specifically, let $\mathbf{u}_0$ be fixed and consider the map

$$\gamma \to \phi_\infty(\mathbf{u}_0, \gamma), \qquad \text{for} \quad \gamma > 0. \tag{5.4}$$

Then this map is piecewise continuous and for every $\mathbf{u}_0 \in \mathbb{R}^2,\ \mathbf{u}_0 \neq (0,0)$, the set of discontinuities is nonempty. This allows us to define the set of discontinuities of the map $\phi_\infty(\mathbf{u}_0, \cdot)$ and order this set. Therefore, we define

$$S(\mathbf{u}_0) \stackrel{\text{def}}{=} \{\hat{\gamma}_k : \phi_\infty(\mathbf{u}_0, \cdot) \text{ is discontinuous at } \gamma = \hat{\gamma}_k\}. \tag{5.5}$$

We define the set $S(\mathbf{u}_0)$ in such a way that the discontinuity values $\hat{\gamma}_k$ are ordered increasingly. We know that $S(\mathbf{u}_0)$ is nonempty and it could consist of one value.

The set $S(\mathbf{u}_0)$ varies with $\mathbf{u}_0$. In the next plot we show this; we have chosen $\alpha = 0.7$ but as initial data we have now chosen $\mathbf{u}_0 = (1, \frac{1}{5})$. We show that in this case the discontinuity in the final equilibrium $\phi_\infty(\mathbf{u}_0, \cdot)$ occurs for some value $\hat{\gamma} \in (0.48, 0.485)$, but that $\phi_\infty(\mathbf{u}_0, \gamma)$ is continuous on the interval $(0.47, 0.48)$, while in the previous case (5.3) a discontinuity occurred on the interval $(0.47, 0.48)$. We also note that the jump occurs at some value slightly higher or equal to γ_*^- and lower than $\frac{1}{2}$.

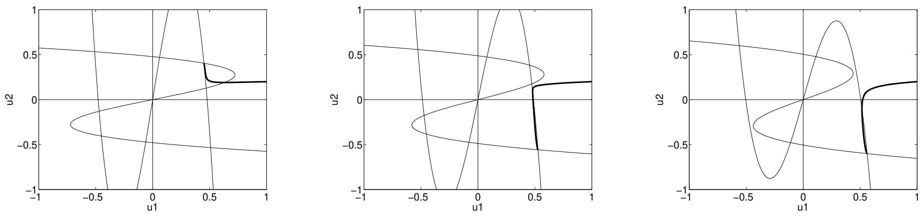

(a) $\gamma = 0.485$. (b) $\gamma = 0.48$. (c) $\gamma = 0.47$.

Figure 15: Graphs of the isoclines and orbits for $\alpha = 0.7$ and $u_0 = \left(1, \frac{1}{5}\right)$

Let us finish by a lemma that can help us to describe the dynamics and determine the final profile in some sets. We define the quadrants

$$\begin{aligned}
Q_1 &\stackrel{\text{def}}{=} \left\{(u_1, u_2) \in \mathbb{R}^2 : u_1 > 0 \text{ and } u_2 > 0\right\}, \\
Q_2 &\stackrel{\text{def}}{=} \left\{(u_1, u_2) \in \mathbb{R}^2 : u_1 < 0 \text{ and } u_2 > 0\right\}, \\
Q_3 &\stackrel{\text{def}}{=} \left\{(u_1, u_2) \in \mathbb{R}^2 : u_1 < 0 \text{ and } u_2 < 0\right\}, \\
Q_4 &\stackrel{\text{def}}{=} \left\{(u_1, u_2) \in \mathbb{R}^2 : u_1 > 0 \text{ and } u_2 < 0\right\}.
\end{aligned}$$

Lemma 5.1

1. *For $\gamma > \frac{1}{2}$, the quadrants Q_1 and Q_3 are positively invariant.*

2. *For $\gamma < \frac{1}{2}$, the quadrants Q_2 and Q_4 are positively invariant.*

This lemma is easily proved by inspection of the vector field on the boundary of the quadrants. Note that in each quadrant we have at most one stable equilibrium. Therefore, this lemma can determine the final profile $\phi_\infty(\mathbf{u}_0, \gamma)$ for different values of γ and $\mathbf{u}_0$ and the discussion is considerably reduced.

In the next section we will try to give the global picture of the dynamics and reformulate the question about the discontinuities of the map in (5.4). Theorem 4.3 will be an important ingredient in the discussion.

6 Phase plane analysis and large time behavior

Let us describe what we are going to do. First, we recall Theorem 4.3 and the critical values found there. We study the different intervals and give a global picture of the dynamics via a phase-plane argument. Then, we make a few observations and we formulate the claim of Proposition 6.1. This allows us to give a different characerization of the set $S(\mathbf{u}_0)$ of discontinuities of the map (5.4).

We want to emphasize that the numerical simulations of last section have been the main motivation for this one. The section has been devoted to describe some relevant phenomena, in particular, the dependence of $\phi_\infty(\mathbf{u}_0, \gamma)$ with respect to $\mathbf{u}_0$ and γ and the observed discontinuities. Our intention is mainly descriptive and our approach uses both numerical and analytical arguments. Therefore, we do not pretend to prove rigorously all the statements contained here in the form of "hard" theorems (although we claim it can be done) but understand and describe what is observed and give an outline of the results that stand behind the simulations.

For convenience, let us rewrite the sequece of critical values found in Theorem 4.3: The numerical values were given in (5.2).

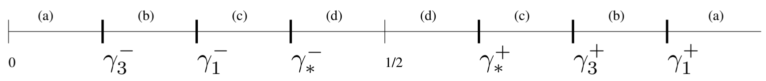

Figure 16: Critical values of γ.

(a) $\boldsymbol{\gamma \in (0, \gamma_3^-) \cup (\gamma_1^+, \infty)}$.

By Theorem 4.3, the origin is globally stable. We plot the stable equilibrium by a circle and the isoclines by dashed lines.

(b) $\boldsymbol{\gamma \in (\gamma_3^-, \gamma_1^-) \cup (\gamma_3^+, \gamma_1^+)}$.

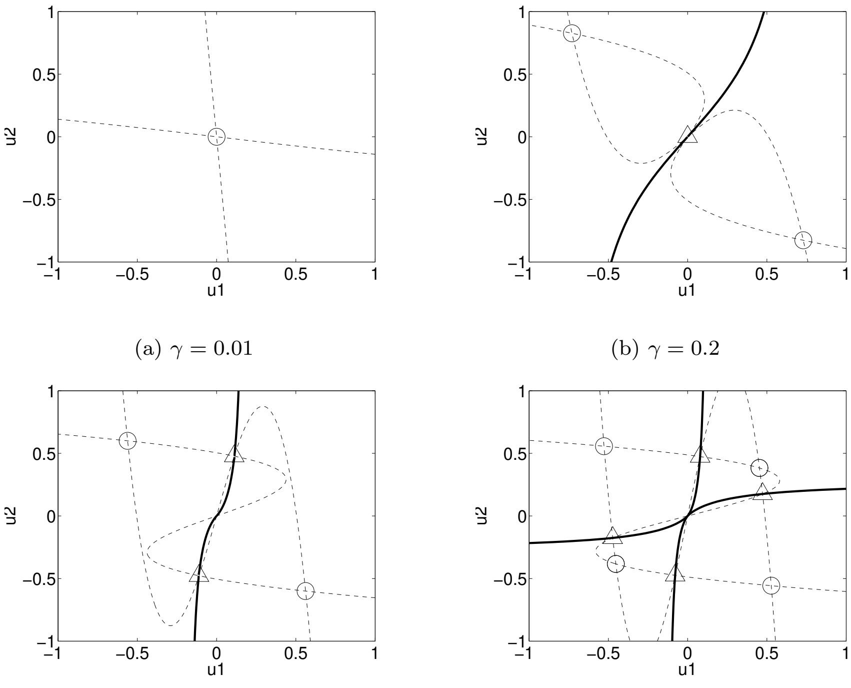

(a) $\gamma = 0.01$

(b) $\gamma = 0.2$

(c) $\gamma = 0.47$

(d) $\gamma = 0.48$

Figure 17: Separatrixes for $\alpha = 0.7$. Circles represent stable nodes and triangles represent saddles.

By Theorem 4.3, the origin is a saddle and we have two stable equilibria P_1 and P_2. We consider the stable manifold of the origin $W_s(0)(\gamma)$. As we know, for fixed γ, $W_s(0)$ is a *separatrix*, so that the complementary set

$$\mathbb{R}^2 - W_s(0) = U_1 \cup U_2,$$

where U_1 and U_2 are two disjoint open sets, each of them containing one different stable equilibrium. Each of them is the domain of attraction of the different equilibria. This is illustrated in Figure 17(b). We plot the stable equilibria by circles, the saddle by a triangle, the isoclines by dashed lines and the separatrix by a thick line.

(c) $\boldsymbol{\gamma \in (\gamma_1^-, \gamma_*^-) \cup (\gamma_*^+, \gamma_3^+)}$.

By Theorem 4.3, the origin is an unstable node and we have two stable equilibria $P_1,\ P_2$ and two saddles $P_3,\ P_4$. Consider the set $W_s(P_3) \cup W_s(P_4)$. Again, the complementary set satisfies

$$\mathbb{R}^2 - \left\{W_s(P_3) \cup W_s(P_4)\right\} = U_1 \cup U_2 \cup \{(0,0)\},$$

where U_1 and U_2 are two disjoint sets, each of them being the domain of attraction of one stable equilibrium. This is illustrated in Figure 17(c).

(d) $\boldsymbol{\gamma \in (\gamma_*^-, \gamma_*^+)}$.

By Theorem 4.3, the origin is an unstable node and we have four stable equilibria $P_1,\ P_2,\ P_3,\ P_4$ and four saddles $P_5,\ P_6,\ P_7,\ P_8$. As before, we consider the set $\cup_{i=5}^{8} W_s(P_i)$. The complemantary set satisfies

$$\mathbb{R}^2 - \bigcup_{i=5}^{8} W_s(P_i) = \bigcup_{i=1}^{4} U_i \cup \{(0,0)\}\,.$$

where the sets U_i are disjoint, each of them being the domain of attraction of P_i for each $1 \leqslant i \leqslant 4$. This is illustrated in Figure 17(d)

For $\gamma > 0$, we define the map

$$\gamma \to \Lambda(\gamma) \stackrel{\text{def}}{=} \bigcup_i \{W_s(P_i) : P_i \text{ is a saddle }\}\,. \tag{6.1}$$

In Figure 17 we represent with a thick line the set $\Lambda(\gamma)$ for different values of γ and fixed $\alpha = 0.7$.

We will now reformulate the question about the discontinuity of the map (5.4) and describe the set $S(\mathbf{u}_0)$, defined in (5.5), in terms of the set $\Lambda(\gamma)$.

Let $\mathbf{u}_0 \in \mathbb{R}^2,\ \mathbf{u}_0 \neq (0,0)$ be fixed. For any $\gamma > 0$, if $\mathbf{u}_0 \in W_s(P_i)$ for some saddle P_i, then $\phi_\infty(\mathbf{u}_0, \gamma) = P_i$. Otherwise, there exists a unique U_i such that $\mathbf{u}_0 \in U_i$, the domain of attraction of some stable equilibrium P_i, and $\phi_\infty(\mathbf{u}_0, \gamma) = P_i$.

Let $\gamma_0 > 0$ be a noncritical value, $\mathbf{u}_0 \neq (0,0)$ be fixed and suppose that $\mathbf{u}_0 \in U_i$ for some index i. Then, $\mathbf{u}_0 \in U_i$ for all $\gamma \in (\gamma_0 - \varepsilon, \gamma_0 + \varepsilon)$ for some $\varepsilon > 0$. Therefore, the map (5.4) is continuous at $\gamma = \gamma_0$. In other words, leaving the critical values apart, we can characterize the set $S(\mathbf{u}_0)$ as follows

Proposition 6.1 *Let γ be a noncritical value. Then, we have*

$$\gamma \in S(\mathbf{u}_0) \textit{ if and only if } \mathbf{u}_0 \in \Lambda(\gamma).$$

Let γ_0 be fixed. Since the domain of attraction U_i of a stable node is open, the map (5.4) is continuous at $\gamma = \gamma_0$ for any $\mathbf{u}_0 \in U_i$. Hence, a discontinuity can only occur at points $\mathbf{u}_0$ contained in a stable manifold of a saddle. To prove the other implication, we need to prove that $S(\mathbf{u}_0)$ is a set of isolated values. A sufficient condition is that for every noncritical $\gamma > 0$ and every $\mathbf{u} \in \Lambda(\gamma)$, the vector flow $\frac{d}{d\gamma}\Lambda(\gamma)$ is transversal to $\Lambda(\gamma)$.

Proposition 6.1 gives us an alternative way to describe $S(\mathbf{u}_0)$, by checking if $\mathbf{u}_0 \in W_s(P_i)$ for some saddle P_i. The definition is more handy when $\mathbf{u}_0$ is fixed and γ varies; the alternative is more handy when γ is fixed. In the latter case, we study the evolution of a finite number of orbits, that is, the stable manifolds of the saddles, with respect to γ.

Proposition 6.1 deals with noncritical values of γ. Let us consider the critical ones. We will distinguish a first group of critical values $\gamma_3^-, \gamma_1^-, \gamma_3^+, \gamma_1^+$, for which the spectrum of the linearised operator around the origin contains the zero eigenvalue, and a second group consisting of γ_*^- and γ_*^+. This latter group corresponds to the critical values for which a *saddle-node bifurcation* occurs, and the number of stable equilibria changes when γ crosses them, in contrast to the first group. The reason for this distinction can become apparent by looking at the series of plots in Figure 17. The main difference is found in the evolution of the separatrix. We will try to describe it now.

Proposition 6.2

1. *Proposition 6.1 holds for* $\gamma \in \{\gamma_3^-, \gamma_1^-, \gamma_3^+, \gamma_1^+\}$.
2. *Proposition 6.1 does not hold for* $\gamma \in \{\gamma_*^-, \gamma_*^+\}$.

Let us start with the first group. We recall that these are the critical values for which the spectrum of the linearised operator around the origin contains the zero eigenvalue. In fact, for these critical values, Proposition 6.1 can be shown to hold.

Let us consider first the case $\gamma = \gamma_3^-$ and $\gamma = \gamma_1^+$. The evolution can be observed by comparing Figures 17(a) and 17(b). For $\gamma < \gamma_3^-$ and $\gamma > \gamma_1^+$, the set $\Lambda(\gamma)$ is empty. When γ crosses these values, the origin becomes a saddle and the separatrix arises, but two stable equilibria bifurcate from the origin.

Next, let us consider the case $\gamma = \gamma_3^+$ and $\gamma = \gamma_1^-$. The evolution can be observed by comparing Figures 17(b) and 17(c). When γ crosses these values, the origin becomes an unstable node and two new saddles bifurcate from the origin, but the map defined in (6.1) is continuous. Therefore, Proposition 6.1 also holds for these values of γ.

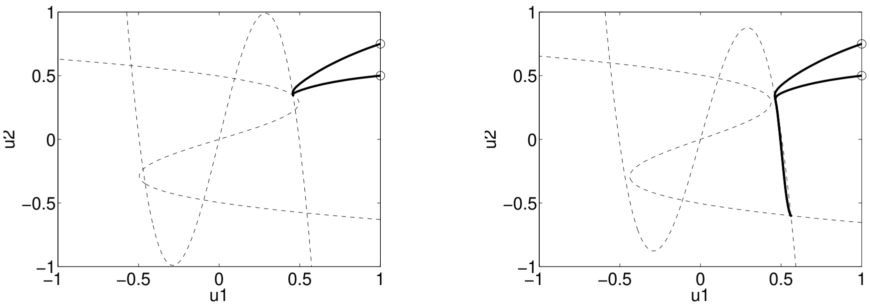

(a) $\gamma = 0.475$. (b) $\gamma = 0.47$.

Figure 18: Graphs of the orbits for equation (5.1) with conditions given by (6.2).

Finally, the values γ_*^- and γ_*^+ are qualitatively different and that can be observed by comparing Figures 17(c) and 17(d). For $\gamma \in [\gamma_3^-, \gamma_*^-) \cup (\gamma_*^+, \gamma_1^+]$ $\Lambda(\gamma)$ consists of two orbits, while for $\gamma \in [\gamma_*^-, \gamma_*^+]$, $\Lambda(\gamma)$ consists of four orbits.

Let $\gamma \in [\gamma_*^-, \gamma_*^+]$ and for every $1 \leqslant i \leqslant 4$ define $P_i(\gamma)$ as the unique stable node found in the i-th quadrant Q_i and let $U_i(\gamma)$ be its domain of attraction. Then, we have $U_1(\gamma_*^-) = \lim_{\gamma \searrow \gamma_*^-} U_1(\gamma)$. Let $\mathbf{u}_0 \in U_1(\gamma_*^-)$. Then there exists some $\varepsilon > 0$ such that

$$\begin{array}{lll} \phi_\infty(\mathbf{u}_0, \gamma) = P_4(\gamma) & \text{for every} & \gamma \in (\gamma_*^- - \varepsilon, \gamma_*^-) \quad \text{and} \\ \phi_\infty(\mathbf{u}_0, \gamma) = P_1(\gamma) & \text{for every} & \gamma \in [\gamma_*^-, \gamma_*^- + \varepsilon). \end{array}$$

In particular, $\gamma_*^- \in S(\mathbf{u}_0)$ and $\mathbf{u}_0$ is not contained in the stable manifold of any saddle, so Proposition 6.1 does not hold for γ_*^-. A similar argument can be used for γ_*^+.

We can see this last property in Figure 18. We have plotted the orbit for equation (5.1), with

$$\alpha = 0.7 \quad \text{and initial data } \mathbf{u}_0 = \left(1, \frac{1}{2}\right), \text{ and } \quad \mathbf{u}_0 = \left(1, \frac{3}{4}\right) \tag{6.2}$$

Both initial data are contained in $U_1(\gamma_*^-)$ and they are shown by a circle. We plot the isoclines with dashed lines and the orbits with thick line. For $\gamma = 0.475$, $\phi_\infty(\mathbf{u}_0) = P_1$ while for $\gamma = 0.47$, $\phi_\infty(\mathbf{u}_0) = P_4$. Note that this case is different from the case shown in Figure 15, where the initial data was $\mathbf{u}_0 = \left(1, \frac{1}{5}\right)$. There, the discontinuity occurs for a noncritical value. The reason is that $\mathbf{u}_0 = \left(1, \frac{1}{5}\right) \notin U_1(\gamma_*^-)$.

Appendix

A Proof of Theorem 3.1

Theorem A.1 *The number of symmetric equilibria of equation* (2.1) *is given by:*

1. *If* $0 < \sigma < 2 - \sqrt{2}$*, then the origin is the unique equilibrium. It is stable.*

2. *If* $2 - \sqrt{2} < \sigma < 2 + \sqrt{2}$*, then there exist two nontrivial symmetric equilibria. They bifurcate from the origin at* $\sigma = 2 - \sqrt{2}$ *(supercritical pitchfork bifurcation) into the first and the third quadrant and they extend to* $\sigma =, \infty$*. They are stable nodes for every* $\sigma > 2 - \sqrt{2}$ *and in this regime, the origin is a saddle.*

3. *If* $2 + \sqrt{2} < \sigma < \hat{\sigma}$*, then there exist four nontrivial equilibrium states. The two new symmetric equilibria bifurcate from the origin at* $\sigma = 2 + \sqrt{2}$ *(supercritical pitchfork bifurcation) into the second and the fourth quadrant, and they extend to* $\sigma = \infty$*. They are saddles for every* $\sigma > 2 + \sqrt{2}$ *and the origin becomes an unstable node.*

4. *If $\sigma > \hat{\sigma}$, then there exist eight nontrivial equilibria. The four new symmetric equilibria emerge at $\sigma = 2 + \hat{\mu}$ from a saddle-node bifurcation at a point in the second, respectively the fourth, quadrant. The equilibrium states with the highest value of $|u_2|$ are stable nodes and the other two are saddles.*

Proof. We are searching for symmetric equilibria of equation (2.1a). That is equivalent to solving the following system

$$\begin{cases} x_2 - 2x_1 + \sigma f(x_1) & = 0, \\ 2x_1 - 2x_2 + \sigma f(x_2) & = 0. \end{cases} \tag{A.1}$$

Let us make some preliminary observations about system (A.1). The origin is a solution for every σ. By the odd symmetry of f, if (x_1, x_2) solves (A.1), so $(-x_1, -x_2)$ does, and if we put $x_1 = 0$ in (A.1), we obtain the origin as the unique solution. This allows us to restrict our search for nontrivial equilibria on $x_1 > 0$. Moreover, for $\sigma = 0$, the origin is the unique solution of system (A.1), so we can restrict to $\sigma > 0$. Therefore, we will search for nontrivial equilibria of (A.1) in the set

$$U \stackrel{\text{def}}{=} \left\{ \big(\sigma, x_1, x_2\big) \in \mathbb{R}^3 : \sigma > 0, \quad x_1 > 0 \right\}.$$

In Figure 2 we have plotted the isoclines for different values of σ, so that we can obtain a geometric view of the system. For small $\sigma > 0$, the isoclines intersect only at the origin. The value $\sigma = 2 - \sqrt{2}$ is the bifurcation value since the slopes of both isoclines equalize. At $\sigma = 2$, both isoclines have negative slope at the origin and eventually, at $\sigma = 2 + \sqrt{2}$, both slopes coincide again. These cases correspond to equilibria bifurcating from the origin. Finally, at $\sigma = 2 + \hat{\mu}$, a saddle-node bifurcation occurs.

Let us give an overview of the strategy we will follow. We will convert system (A.1) into one single polynomial equation for x_1 of degree 8. Then we will transform this equation into a simpler equation (A.4). This is a polynomial of degree 4 for a new variable p. The transformation of both problems is carried out in (A.3). Therefore, searching for solutions of equation (A.1) in the set U is equivalent to searching for solutions of equation (A.4) in the following set

$$V \stackrel{\text{def}}{=} \left\{ (p, \mu) \in \mathbb{R}^2 : \mu > -2, \quad p + \mu > 0 \right\}.$$

This problem can be solve analytically: we can find an open set $\mathcal{O} \subset \mathbb{R}$ such that the solutions of (A.4) in V correspond to a graph $\big(p, \mu(p)\big)$ defined on $p \in \mathcal{O}$. Finally, we draw the corresponding conclusions in terms of the original variables x_1, x_2 and parameter σ.

We start our procedure by solving the first equation of system (A.1) for x_2 and substitute in the second one. This gives us one single polynomial equation for x_1.After division by x_1 we obtain

$$\sigma^4 x_1^8 - 3\sigma^3(\sigma-2)x_1^6 + 3\sigma^2(\sigma-2)^2 x_1^4 - \sigma(\sigma-2)\left\{1 + (\sigma-2)^2\right\} x_1^2 + (\sigma-2)^2 - 2 = 0. \tag{A.2}$$

To simplify the analysis, we make the following transformation,

$$\begin{array}{rcl} \mu & = & \sigma - 2, \\ p & = & \sigma x_1^2 + 2 - \sigma = (2+\mu)x_1^2 - \mu. \end{array} \tag{A.3}$$

Then equation (A.2) is equivalent to

$$g(\mu, p) \stackrel{\text{def}}{=} p^4 + \mu p^3 - \mu p - 2 = 0. \tag{A.4}$$

Since we look for solutions in the set$U$, this implies that we are searching for pairs (p, μ) such that

$$\mu > -2, \quad p + \mu > 0 \tag{A.5}$$

Note that $\sigma = 2 + \mu > 0$. Therefore, we search for solutions in V.

We can explicitly solve equation (A.4) for μ. This yields

$$\mu(p) = \frac{2 - p^4}{p^3 - p}. \tag{A.6}$$

We search for pairs $\big(p, \mu(p)\big) \in V$ satisfying equation (A.6) and inequalities (A.5). Easy analysis shows that this holds iff $p \in \mathcal{O} \stackrel{\text{def}}{=} (-\infty, -\sqrt{2}) \cup (-1, 0) \cup (1, \sqrt{2})$.

In Figure 19 we plot the graph of the function $\mu(p)$ in the set $p \in \mathcal{O}$. The dashed plot represents the boundaries of the inequalities (A.5), that is, the graphs of $\mu = -p$ and $\mu = -2$. Recall that by (A.5), only the part of the plot above them is admissible.

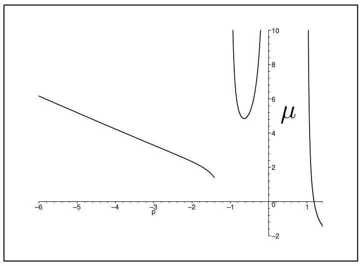

Figure 19: Plot of $\mu(p)$ in the admissible set $\mathcal{O}$.

The graph is as follows: for $p \in (-\infty, -\sqrt{2})$, $\mu(p)$ decreases from ∞ to $\sqrt{2}$. For $p \in (-1, 0)$, $\mu(p)$ decreases from ∞ to the local minimum $\hat{\mu}$ and it increases back to ∞. For $p \in (1, \sqrt{2})$, $\mu(p)$ decreases from ∞ to $-\sqrt{2}$.

Let us draw the conclusions in terms of the parameter μ. For μ close to -2, there exist no nontrivial equilibrium. At $\mu = -\sqrt{2}$, the first branch of equilibria bifurcates from the origin and they are well defined for every $\mu \geqslant -\sqrt{2}$. At $\mu = \sqrt{2}$, a second branch bifurcates from the origin and they are well defined for every $\mu \geqslant \sqrt{2}$. At $\mu = \hat{\mu}$, two branches emerge from a nontrivial equilibrium (saddle-node bifurcation) and they are defined for every $\mu \geqslant \hat{\mu}$.

Note that the value $\hat{\mu}$ can be found as the local minimum for $\mu(p)$ in the interval $p \in (-1, 0)$. It can be alternatively found by solving the system:

$$\left\{ \begin{array}{rcl} g(\mu, p) & = & 0, \\ \frac{\partial g}{\partial p}(\mu, p) & = & 0. \end{array} \right. \tag{A.7}$$

We can give an analytic expression of the bifurcation branches $\big(\sigma, x_1(\sigma)\big)$ with parametric coordinates:

1. First branch:

$$\sigma(p) = 2 + \mu(p), \quad x_1(p) = \pm\sqrt{\frac{p + \mu(p)}{2 + \mu(p)}} \qquad \text{for} \quad 1 < p < \sqrt{2}.$$

2. Second branch:

$$\sigma(p) = 2 + \mu(p), \quad x_1(p) = \pm\sqrt{\frac{p + \mu(p)}{2 + \mu(p)}} \qquad \text{for} \quad p < -\sqrt{2}.$$

3. Third branch:

$$\sigma(p) = 2 + \mu(p), \quad x_1(p) = \pm\sqrt{\frac{p + \mu(p)}{2 + \mu(p)}} \qquad \text{for} \quad -1 < p < 0.$$

References

[1] R. Aris: The Mathematical Theory of Diffusion and Reaction in Permeable Catalysts, *Clarendon Press*, Oxford, 1975.

[2] D. G. Aronson and L. A. Peletier: Global stability of symmetric and asymmetric concentration profiles in catalyst particles, *Arch. Rational Mech. Anal.* **54** (1974), 175–204.

[3] N. Chafee and E. F. Infante: Bifurcation and stability for a nonlinear parabolic partial differential equation, *Bull. Amer. Math. Soc.* **80** (1974), 49–52.

[4] P. Collet and J. P. Eckmann: Instabilities and fronts in extended systems, *Princeton University Press, Princeton Series in Physics*, 1990.

[5] J. K. Hale: Asymptotic behaviour of dissipative systems, *Mathematical Surveys and Monographs* **25**, AMS, Providence, 1988.

[6] L. Kramer and P. C. Hohenberg: Effects of boundary conditions on spatially periodic states, *Phys. D* **13** (1984), 357–369.

[7] L.A. Peletier and V. Rottschäfer: Large time behaviour of solutions of the Swift-Hohenberg equation, *C.R. Acad. Sci. Paris, Ser. I* **336** (2003), 225–230.

[8] L. A. Peletier and V. Rottschäfer: Pattern selection of solutions of the Swift-Hohenberg equation, Leiden university, preprint.

[9] L.A. Peletier and W.C. Troy: Higher order models in Physics and Mechanics, Birkhäuser, Boston, 2001.